



Title	Upon the limit of the elastic buckling : principally about the steel column
Author(s)	Kon, Toshizo
Citation	Memoirs of the Faculty of Engineering, Hokkaido University, 8(3-1), 67-103
Issue Date	1950-12-20
Doc URL	<a href="http://hdl.handle.net/2115/37764">http://hdl.handle.net/2115/37764</a>
Type	bulletin (article)
File Information	8(3-1)_67-103.pdf



[Instructions for use](#)

# Upon the Limit of the Elastic Buckling (Principally about the Steel Column)

Toshizo KON

(Received Dec. 23, 1949.)

## Synopsis

The main and initiated object of the present research is to inquire about the influence of the grade of elastic material upon the strength of elastic buckling of a column, which existence was considered negative for a long time since Euler. Through the acquirement of the comparatively simple relation between the column load and its flexure from the exact elliptic-functional one in this study, the important properties concerning with the unknown field of elastic buckling have been made clear. Namely, pointing out some of the results, the elastic buckling is perfectly possible to occur under the intense flexure of a column if its slenderness ratio is provided to be sufficiently great; the grade of material makes a remarkable influence upon the strength of elastic buckling of a column whose slenderness ratio is sufficiently great, which the Euler's theory could never acknowledge hitherto; even the column of an infinite slenderness ratio is resistible to a certain amount of the column load which is finite, and its amount is peculiar to the grade of material and the type of cross-section; the type of cross-section effects the buckling stress notably under the slenderness ratio mentioned above, and the column of composite section where the radius of gyration is so efficient is more resistible elastically to the intense flexure due to buckling than that of solid one; for the two modes of buckling subject to the case of an unsymmetrical cross-section, both buckling stresses due to the compressive extreme fibre stress and tensile one reaching the limit of proportionality can be observed as nearly equal through the result of computation. Finally, for the region of practice about the elastic buckling where the slenderness ratio is not so great, the classical law of Euler and the author's can be seen as approximately coincident each other. Thus, the Euler's theory shall be recognized as the law of the lower limiting boundary of the domain where the elastic buckling is possible, while the author's one makes the upper limiting boundary of the same domain, concerning the buckling stress.

Through the comparative calculation about St 37 and St 52 according to the present new theory, the author has treated and discussed above problems and conclusions in detail.

## 1. Introduction

The Euler's classical law of the elastic buckling defines the relation between the stress and the slenderness ratio of a column which undergoes a concentric load, at the moment when it starts to begin a flexure in the column; or, this expresses the uppermost load in the state of stable equilibrium of an unflexured, straight column, on the region of the elastic buckling. The magnitude of this flexure becomes greater, for the first time, according to the growth of the column load  $P$  beyond the Euler's critical one  $P_k$ , but so far as the maximum fibre stress introduced at the compressive or tensile side of the flexured column does not exceed the limit of proportionality  $\sigma_p$  of the material, the column shall be considered to be still under the state of the elastic buckling and of the stable equilibrium in flexure. Therefore, satisfying such a critical condition, we can obtain the relation between the load (or the stress intensity) and the slenderness ratio of a column for the region of the elastic buckling beyond the critical boundary which was founded by Euler, and the load such a theory will give must be greater than that the Euler's gives for a definite slenderness ratio, as may be expected evidently. Through this process, we can make clear the properties of the elastic buckling perfectly, in the more widened field of the column problem than before, and it may offer us the fact that the problem of the elastic buckling should have involved, not only the modulus of elasticity as claimed classically, but also the limit of proportionality as the serious factor relating materials, which result ought to be said as of a great significance technologically. On the present treatise, the author has investigated the problem above mentioned for steel columns with cross-sections which are common in the bridge practice, discussing about the meaning of the Euler's law in relation with the new theory of this research.

## 2. Theory

The differential equation of the elastic buckling beyond the Euler's load is written as (Fig. 1)

$$\frac{y'''}{\sqrt{1 + y'^2}} + \kappa y = 0 \dots\dots\dots (1)$$

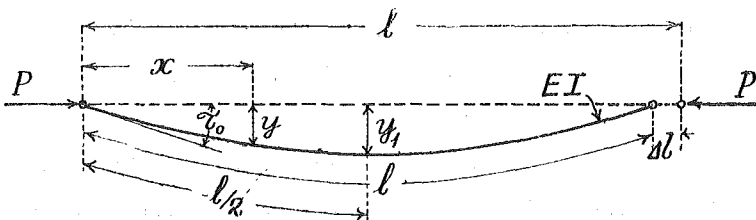


Fig. 1

where it denotes  $EI$  : the flexural rigidity, and  $\kappa = \frac{P}{EI}$ ,  
 $\tau_o$  : the slope of the tangent to the end of a flexured column,  
 $y_1$  : the maximum deflection,  
 $\Delta l$  : the mutual displacement of both ends of column in direction of the unflexured column axis.

Integrating (1) by  $y$ , we obtain

$$-\frac{1}{\sqrt{1+y'^2}} + \frac{\kappa}{2} y^2 + c = 0 \dots\dots\dots (2)$$

where  $c$  means the unknown quantity  $\cos \tau_o$ . As the equation (2) gives the relation

$$\frac{dy}{dx} = \frac{\sqrt{1 - \left(\frac{\kappa}{2} y^2 + c\right)^2}}{\frac{\kappa}{2} y^2 + c},$$

it results

$$ds = \frac{dy}{\sqrt{1 - \left(\frac{\kappa}{2} y^2 + c\right)^2}} \dots\dots\dots (3).$$

At the point of the maximum deflection  $y_1$ , it becomes  $y' = 0$ . Hence, quantities  $y_1$  and  $c$  will be related as follows :

$$y_1 = \sqrt{\frac{2}{\kappa} (1-c)} \dots\dots\dots (4).$$

Now, substituting  $z = \frac{y}{y_1}$  ( $z < 1$ ), the right side of equation (3) can be written as

$$\frac{dy}{\sqrt{1 - \left(\frac{\kappa}{2} y^2 + c\right)^2}} = \frac{y_1}{\sqrt{1-c^2}} \cdot \frac{dz}{\sqrt{(1-z^2)(1-k^2 z^2)}}$$

where

$$k^2 = -\frac{1-c}{1+c}, (c < 1) \dots\dots\dots (5);$$

and, as it is  $\frac{y_1}{\sqrt{1-c^2}} = \sqrt{\frac{1-k^2}{\kappa}}$ , the equation (3) follows as

$$ds = \sqrt{\frac{1-k^2}{\kappa}} \cdot \frac{dz}{\sqrt{(1-z^2)(1-k^2 z^2)}} \dots\dots\dots (6).$$

The integration of the equation (6) along the flexured half column-axis from  $o$  to  $\frac{l}{2}$  corresponds to that from  $o$  to  $y_1$  of the deflection, and so we obtain the

equation

$$\frac{l}{2n} = \sqrt{\frac{\kappa}{1-k^2}} \int_0^1 \frac{dz}{\sqrt{(1-z^2)(1-k^2 z^2)}} \dots\dots\dots (7),$$

or expressing symbolically

$$\frac{l}{2n} \sqrt{\frac{\kappa}{1-k^2}} = \mathbf{K} \dots\dots\dots (8);$$

$n$  means the order of buckling, i. e. the number of deflected waves contained in the flexured column, and  $\mathbf{K}$ , the complete elliptic integral of first sort with the negative modulus  $k^2$ . If the modulus  $k^2$  is given,  $\mathbf{K}$  can be computed by the relation

$$\mathbf{K} = \int_0^1 \frac{dz}{\sqrt{(1-z^2)(1-k^2 z^2)}} = \frac{\pi}{2} \left[ 1 + \left(\frac{1}{2}\right)^2 k^2 + \left(\frac{1.3}{2.4}\right)^2 k^4 + \left(\frac{1.3.5}{2.4.6}\right)^2 k^6 + \dots\dots\dots \right] \dots\dots\dots (9)^*.$$

From this, we get

$$(1-k^2) \left(\frac{2}{\pi} \mathbf{K}\right)^2 = 1 - \frac{1}{2} k^2 - \frac{5}{32} k^4 - \frac{5}{64} k^6 - \frac{389}{8192} k^8 - \dots (10),$$

and substituting (8) into (10), and through some transformation, the following can

be attained

$$\nu_1^2 = 1 - \frac{1}{2} k^2 - \frac{5}{32} k^4 - \frac{5}{64} k^6 - \frac{389}{8192} k^8 - \dots\dots\dots$$

with notations

$$\nu_1^2 = \frac{\kappa l^2}{n^2 \pi^2} = \frac{P}{n^2 P_k} = \frac{\nu^2}{n^2}$$

where  $\nu^2 = \frac{P}{P_k} (\nu^2 > 1)$ ,

$$P_k = \frac{\pi^2 EI}{l^2} \text{ (Euler's critical load).}$$

} (11)

Now, expressing the modulus  $k^2$  through  $\nu_1$  reversely, we get an infinite series in  $\nu_1$  as follows

$$k^2 = -2(\nu_1^2 - 1) \left[ 1 + \frac{5}{8} (\nu_1^2 - 1) + \frac{5}{32} (\nu_1^2 - 1)^2 + \frac{7}{256} (\nu_1^2 - 1)^3 + \dots\dots\dots \right] \dots\dots\dots (12),$$

which series defines the modulus of the above elliptic integral in the case of elastic buckling due to the concentric column load  $P$ . Besides, the quantity  $c$  will be expressed through  $\nu_1$  also :

\* Jahnke-Emde : Funktionentafeln.

$$c = \cos \tau_o = \frac{1 + k^2}{1 - k^2} = \frac{1 - 2(\nu_1^2 - 1) \left[ 1 + \frac{5}{8}(\nu_1^2 - 1) + \frac{5}{32}(\nu_1^2 - 1)^2 + \frac{7}{256}(\nu_1^2 - 1)^3 + \dots \right]}{1 + 2(\nu_1^2 - 1) \left[ 1 + \frac{5}{8}(\nu_1^2 - 1) + \frac{5}{32}(\nu_1^2 - 1)^2 + \frac{7}{256}(\nu_1^2 - 1)^3 + \dots \right]} \dots \dots \dots (13).$$

Thus, with the expression (13) for  $c$  in hand, the maximum ordinate of flexure  $y_1$  has become to be able to express through  $\nu_1$  from (4), as follows, considering, however, the case of the first order ( $n = 1$ ) merely,

$$y_1 = \frac{l}{\pi \nu} \phi(\nu)$$

where

$$\phi(\nu) = \sqrt{\frac{8(\nu^2 - 1) \left[ 1 + \frac{5}{8}(\nu^2 - 1) + \frac{5}{32}(\nu^2 - 1)^2 + \frac{7}{256}(\nu^2 - 1)^3 + \dots \right]}{1 + 2(\nu^2 - 1) \left[ 1 + \frac{5}{8}(\nu^2 - 1) + \frac{5}{32}(\nu^2 - 1)^2 + \frac{7}{256}(\nu^2 - 1)^3 + \dots \right]}} \dots \dots (14).$$

This mathematical result (14) for  $y_1$ , which the author has successfully introduced in a very easy but generalized algebraic form of  $\nu$ , enables us to obtain the exact middle deflection of the column which is concentrically loaded with any load  $P$  greater than  $P_k$ , and offers the serious first step to pioneer the widened field for the problem of the elastic buckling.

From the equation (12), its infinite series on the right side can be transformed as

$$1 + \frac{5}{8}(\nu^2 - 1) + \frac{5}{32}(\nu^2 - 1)^2 + \dots = -\frac{k^2}{2(\nu^2 - 1)} = \frac{1}{2(\nu^2 - 1)} \frac{1 - c}{1 + c},$$

whence we have

$$\phi(\nu) = \sqrt{2(1 - c)} \dots \dots \dots (15),$$

or  $c = 1 - \frac{1}{2} \phi^2(\nu) \dots \dots \dots (13a).$

Now, from the equation (13), the special values of  $c$  are got, *i. e.* :

for  $\nu^2 = 1, \quad c = 1 \quad (\tau_o = 0)$  and for  $\nu^2 = \infty, \quad c = -1$   
 $(\tau_o = \pi),$

which correspond from (15),

for  $\nu^2 = 1, \quad \phi(\nu) = 0$  and for  $\nu^2 = \infty, \quad \phi(\nu) = 2.$

Thus, since the function  $\phi(\nu)$  conveges to a certain value between 0 and 2

corresponding to the variation of  $\nu^2$  between unity and infinity (Fig. 2), we know that the equation (14) is applicable for all positive values of  $\nu^2$  greater than unity, and can give a finite numerical value for the deflection  $y_1$ , specified with  $\nu^2$ .

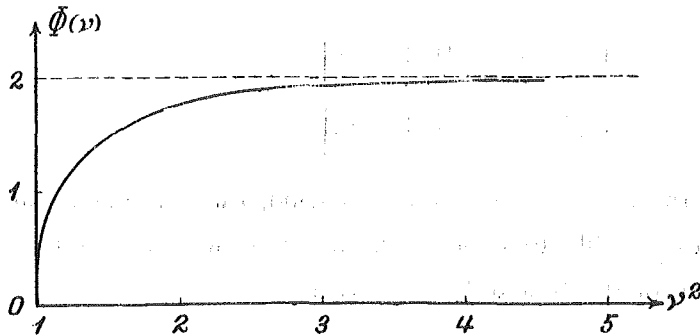


Fig. 2

The equation (14) will give, also, the following one approximately,

$$y_1 = \frac{l}{\pi \nu} \sqrt{\frac{8(\nu^2 - 1)}{1 + 2(\nu^2 - 1)}} = \frac{2l}{\pi \nu} \sqrt{\frac{2(\nu^2 - 1)}{2\nu^2 - 1}} \dots \dots \dots (14a),$$

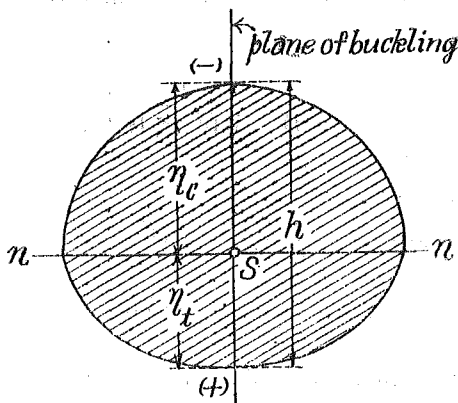
Some authorities, like Grashof, Schneider, v. Mises, Domke,\*<sup>o</sup>) have recommended approximate formulae also, but the above (14a) gives better values than theirs, which are to be written in the notations of the present treatise as follows ;

Grashof,  $y_1 = \frac{2l}{\pi \nu} \sqrt{\nu - 1}$ , or  $= \frac{l}{\pi} \sqrt{\nu^2 - 1}$ ,

Schneider,  $y_1 = \frac{2l}{\pi} \sqrt{2(\nu^2 - 1)}$ ,

v. Mises,  $y_1 = \frac{2l}{\pi \nu} \sqrt{2(\nu^2 - 1)}$ ,

Domke,  $y_1 = \frac{2l}{\pi \nu^2} \sqrt{2(\nu^2 - 1)}$ ,



$W_c = \frac{I}{r_c}$  (-): Compression side  
 (+): Tension side

Fig. 3.

In the flexured column, the maximum bending moment occurs at the middle cross-section and its magnitude is  $P y_1$ ; the compressive extreme fibre stress  $\sigma_2$  due to bending shall be obtained, considering that the Hooke's law is consistent still in this case, Fig.3 :

$$\sigma_2 = \frac{P y_1}{W_c} = \frac{P l \Phi(\nu)}{\pi \nu W_c}$$

\*<sup>o</sup>) Grashof : Theorie der Elastizität u. Festigkeit, 1878, S. 168.  
 Schneider: Zeits. d. Oester. Ing. u. Arch. Vereins, 1901, S. 637.  
 v. Mises: Differentialgleichungen der Physik, I. 1925, S. 376.  
 Domke : Die Bautechnik, 1926, S. 747.

$$= \frac{PI\Phi(\nu)}{\pi\nu I} \eta_c = \sqrt{\frac{EP}{I}} \eta_c \Phi(\nu)$$

or

$$\sigma_2 = \sqrt{\sigma_a E} \frac{\eta_c}{r} \Phi(\nu) \dots \dots \dots (16),$$

where

$$\sigma_a = \frac{P}{A}, \quad r^2 = \frac{I}{A}$$

- A : cross-sectional area,
- r : radius of gyration,
- I : moment of inertia about n-n axis.

Hence, the resultant stress  $\sigma_c$  in the extreme compressive fibre can be written as

$$\sigma_c = \sigma_1 + \sigma_2 = \sigma_a + \sqrt{\sigma_a E} \frac{\eta_c}{r} \Phi(\nu) \dots \dots \dots (17).$$

On the other hand

$$\nu^2 = \frac{\sigma_a \lambda^2}{\pi^2 E} \dots \dots \dots (18),$$

where

the slenderness ratio,  $\lambda = \frac{l}{r}$ ,

which becomes in the special case of the Euler's buckling, as it is  $\nu^2 = 1$ ,

$$\sigma_{\omega E} = \frac{\pi^2 E}{\lambda^2} \dots \dots \dots (18a).$$

As the fundamental criterion for the elastic buckling, we may put, with the limit of proportionality  $\sigma_p$ , as

$$\sigma_a + \sqrt{\sigma_a E} \frac{\eta_c}{r} \Phi(\nu) \leq \sigma_p \dots \dots \dots (19).$$

Or, substituting the equation (18) in this one

$$\frac{\pi^2 E}{\lambda^2} \nu^2 + \frac{\pi E}{\lambda} \nu \frac{\eta_c}{r} \Phi(\nu) \leq \sigma_p \dots \dots \dots (19a).$$

The equation which will be got putting equal both sides of the equation (19a), gives that value of  $\lambda$  at which slenderness ratio the resultant extreme fibre stress in compression attains at the limiting stress  $\sigma_p$  of the elastic buckling, with the given value of  $\nu$  greater than unity. Denoting this slenderness ratio with  $\lambda_{e,p}$ , its solution results as

$$\lambda_{e,p} = \frac{\pi E}{2\sigma_p} \cdot \frac{\eta_c}{r} \nu \Phi(\nu) \left[ 1 + \sqrt{1 + \frac{4\sigma_p}{E\Phi^2(\nu)} \left(\frac{r}{\eta_c}\right)^2} \right] \dots \dots \dots (20)$$

where  $\nu \geq 1$



When the material and the cross-section of a column are given, the quantities  $E, \sigma_p, \eta_c/r$  becomes definite also, and hence, the critical slenderness ratio  $\lambda_{c,p}$  should be obtained from the equation (20) with  $\nu^2$  as the parameter. Consequently, through the equation (18), the buckling column stress  $\sigma_u$  can be obtained corresponding to this slenderness ratio  $\lambda_{c,p}$ .

In the case of Euler's buckling ( $\nu^2 = 1$ ), we specify the slenderness ratio with  $\lambda_p$  instead of  $\lambda_{c,p}$  and the equation (20) gives

$$\lambda_p = \pi \sqrt{\frac{E}{\sigma_p}} \dots\dots\dots (20a).$$

This slenderness ratio  $\lambda_p$  defines the boundary between the regions of the elastic buckling (including the Euler's buckling) and the plastic one, and, also, at this point of the slenderness ratio the Euler's buckling and the laws of the elastic buckling expressed by equation (19) and (20) coincide, and it does never except this point  $\lambda_p$  elsewhere.

Taking steel St 37, as an example, with  $E = 2100 \text{ t/cm}^2$  and  $\sigma_p = 2.1 \text{ t/cm}^2$  we get

$$\lambda_p = \pi \sqrt{\frac{E}{\sigma_p}} = 99.346 \dots\dots\dots (20b),$$

and for steel St 52, with  $\sigma_p = 3.2 \text{ t/cm}^2$ , it becomes

$$\lambda_p = 80.479 \dots\dots\dots (20c).$$

Combining both equation (18) and (20) through  $\lambda$ , the buckling column stress  $\sigma_u$  for the uppermost limit of elastic buckling may be expressed directly by  $\nu$

$$\sigma_u = \frac{4\sigma_p^2}{E} \left(\frac{r}{\eta_c}\right)^2 \frac{1}{\Phi^2(\nu) \left[1 + \sqrt{1 + \frac{4\sigma_p}{E\Phi^2(\nu)} \left(\frac{r}{\eta_c}\right)^2}\right]^2} \dots\dots\dots (21).$$

Since the second term under the radical sign in the denominator is of small quantity against unity, the above formula (21) can be expressed, when the slenderness ratio is fairly great ( $\lambda \cong 400 \sim 500$ ), with the sufficient precision approximately as

$$\sigma_u = \frac{\sigma_p^2}{E} \left(\frac{r}{\eta_c}\right)^2 \frac{1}{\Phi^2(\nu)} \dots\dots\dots (21a).$$

Above formula (21) or (21a) talks the new law of the elastic buckling, and it relates the fact: "The classical law of the Euler's elastic buckling, *i. e.* the eq. (18a), recognizes no superiority of the higher grade material to the lower grade one in the strength of elastic buckling so far as the moduli of elasticity of both materials are same as it is usual in steel: in other words, at the instant when the stable equilibrium in the straight state of the column begins to break, the critical

column loads shall be same for both such materials and indifferent to their grades. When the column load grows beyond the Euler's critical one, the column starts into the state of flexure, but in this flexured state the elastic buckling still exist, conditioned with load, material factors and cross-sectional ones satisfying the equation (21) or (21a) at the uppermost limit; in this case the column should be considered to be in the state of stable equilibrium in flexure. On such a buckling, the circumstance becomes quite different from the former buckling of Euler: the grades of materials remarkably influence the strength of elastic buckling, although their moduli of elasticity are same. Furthermore, even if the moments of inertia were same for columns, the difference in types of cross-section effects the buckling strength notably, also." Thus, through such a law, the theory of elastic buckling seems to be provided with its reasonableness and perfectness.

On the other hand, as it becomes  $\phi(\nu) \rightarrow 2$  for  $\nu^2 \rightarrow \infty$ , the buckling stress  $\sigma_u$  for this case can be derived from the equation (21) as follows,

$$\lim_{\nu^2 \rightarrow \infty} \sigma_u = \lim_{\lambda \rightarrow \infty} \sigma_u = \frac{\frac{\sigma_p^2}{E} \left(\frac{r}{\eta_c}\right)^2}{\left[1 + \sqrt{1 + \frac{\sigma_p}{E} \left(\frac{r}{\eta_c}\right)^2}\right]^2} \dots\dots\dots(22):$$

or approximately

$$\lim_{\nu^2 \rightarrow \infty} \sigma_u = \lim_{\lambda \rightarrow \infty} \sigma_u = \frac{\sigma_p^2}{4 E} \left(\frac{r}{\eta_c}\right)^2 \dots\dots\dots(22a).$$

The equation (22) or (22a) states another new fact: "According to the classical theory of Euler, the column of an infinite slenderness ratio can resist any load no more, and so it is  $\sigma_u = 0$ . The present theory of the author approves that the elastic buckling exists still in this case, and the column of the infinite slenderness ratio is resistible to the load of a certain magnitude, defined by the equations (22) or (22a) and being not zero. In the other words, for the case  $\lambda \rightarrow \infty$ , the quantity  $\sigma_u$  has some asymptote of a particular ordinate whose value varies with the material and the type of cross-section but is not zero."

**3. The theory for the case where the extreme fibre stress reaches to the limit of proportionality sooner upon the tensile fibre than the compressive one.**

When the cross-section of a column is symmetrical about n-n axis (Fig. 3), the absolute maximum normal stress shall never fail to be developed at the compressive extreme fibre of the cross-section; and so, in this case, the limitative stress  $\sigma_p$  of the elastic buckling is to be attained always on the compression side of a

column. Hence, the equations mentioned hitherto, *i. e.* (16), (17), (19), (19a), (20), (21), (21a), (22), (22a), are all applicable for this case. The circumstance is quite

same, also, for the column of an unsymmetrical cross-section, which should buckle so as to satisfy the condition  $\eta_c > \eta_t$ , cf. Fig. 3.

But, when the column of an unsymmetrical cross-section should buckle elastically so that the relation between both edge distances from n-n axis will be held as  $\eta_t > \eta_c$ , the circumstance becomes quite different, and the equations mentioned above shall never be applied for. In such a state of buckling, cf. Fig. 4, the absolute maximum normal stress will be developed at the tensile extreme fibre of the cross-section, and, under a great flexure of the column, this stress will reach to the limit of proportionality certainly. So, another theory is necessary to be derived accomodating to this mode of buckling.

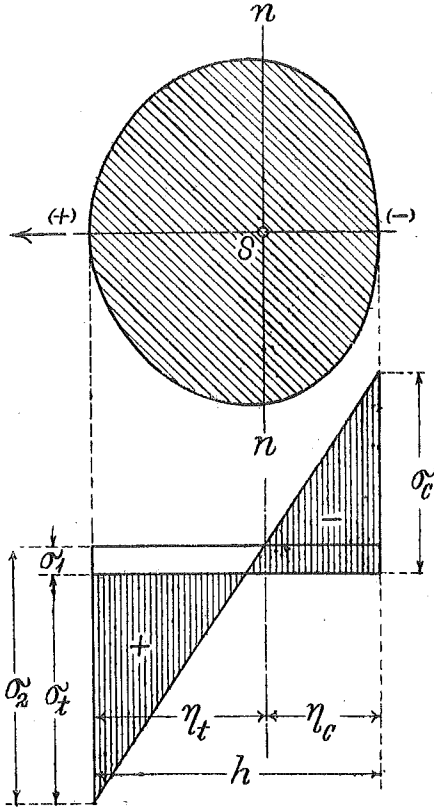


Fig. 4.

Since the maximum normal tensile stress may be written

$$-\sigma_t = \sigma_1 - \sigma_2 = \sigma_{a,+} - \sqrt{\sigma_{a,+} E \frac{\eta_t}{r} \Phi(\nu)}, \dots\dots\dots (23)$$

the fundamental criterion of the elastic buckling for this case will be

$$\sigma_{a,+} - \sqrt{\sigma_{a,+} E \frac{\eta_t}{r} \Phi(\nu)} \leq -\sigma_p \dots\dots\dots (24)$$

denoting with  $\sigma_{a,+}$  the buckling stress  $\sigma_a$  for the mode of buckling in question. Now, substituting the equation (18) in this, we have the following conditional equation

$$\frac{\pi^2 E}{\lambda^2} \nu^2 - \frac{\pi E}{\lambda} \nu \frac{\eta_t}{r} \Phi(\nu) \leq -\sigma_p \dots\dots\dots (24a).$$

Putting both sides of the above equal and solving with  $\lambda$ , it gains the slenderness ratio  $\lambda_{c,p}$  where the extreme fibre stress in tension reaches the limiting stress  $\sigma_p$ ,

$$\lambda_{c,p} = \frac{\pi E}{2\sigma_p} \frac{\eta_t}{r} \nu \Phi(\nu) \left[ 1 + \sqrt{1 - \frac{4\sigma_p}{E \Phi^2(\nu)} \left( \frac{r}{\eta_t} \right)^2} \right] \dots\dots\dots (25),$$

and from equations (25) and (18), the buckling stress can be expressed as

$$\sigma_{a,+} = \frac{\frac{4\sigma_p^2}{E} \left(\frac{r}{\eta_l}\right)^2}{\Phi^2(\nu) \left[1 + \sqrt{1 - \frac{4\sigma_p}{E\Phi^2(\nu)} \left(\frac{r}{\eta_l}\right)^2}\right]^2} \dots\dots\dots(26).$$

The condition that the buckling stress  $\sigma_{a,+}$  shall be real, is gained as

$$\left(\frac{\eta_l}{r}\right)^2 \geq \frac{4\sigma_p}{E\Phi^2(\nu)} \dots\dots\dots(27),$$

which requires the quantity  $\nu^2$  to be sufficiently great. Besides, in such a region of  $\nu^2$ , the equation (26) may be approximately written

$$\sigma_{a,+} = \frac{\sigma_p^2}{E} \left(\frac{r}{\eta_l}\right)^2 \frac{1}{\Phi^2(\nu)} \dots\dots\dots(26a).$$

If the quantity  $\nu^2$  grows infinite, the buckling stress shall converge to the value to be defined by the following equation :

$$\lim_{\nu^2 \rightarrow \infty} \sigma_{a,+} = \lim_{\lambda \rightarrow \infty} \sigma_{a,+} = \frac{\frac{\sigma_p^2}{E} \left(\frac{r}{\eta_l}\right)^2}{\left[1 + \sqrt{1 - \frac{\sigma_p}{E} \left(\frac{r}{\eta_l}\right)^2}\right]^2} \dots\dots\dots(28),$$

or approximately

$$\lim_{\nu^2 \rightarrow \infty} \sigma_{a,+} = \lim_{\lambda \rightarrow \infty} \sigma_{a,+} = \frac{\sigma_p^2}{4E} \left(\frac{r}{\eta_l}\right)^2 \dots\dots\dots(28a).$$

When the quantity  $\nu^2$  satisfies the relation

$$\left(\frac{\lambda_{c,p}}{\nu}\right)_{(-)} = \left(\frac{\lambda_{c,p}}{\nu}\right)_{(+)} \dots\dots\dots(29),$$

the buckling stresses  $\sigma_a$  and  $\sigma_{a,+}$ , defined respectively by the equations (21) and (26), shall become equal, the suffices (-), (+) in the equation (29) expressing the signs of extreme fibre stresses which will grow to the limiting stress  $\sigma_p$  and determine the mode of buckling as referred in the preceding.

Upon the diagram  $\nu^2 - \lambda_{c,p}$ , it becomes simultaneously

$$\nu_{(+)} = \nu_{(-)}, \quad \lambda_{c,p,(+)} = \lambda_{c,p,(-)} \dots\dots\dots(29a)$$

at the conditional point  $\sigma_a = \sigma_{a,+}$ , and the latter condition may never be satisfied at other points, as to be computed and explained in the succeeding diagram.

#### 4. Approximate values for cross-section factors.

In order to start to the computations according to above theoretical equations, it is necessary to know the cross-sectional factors  $\frac{\eta_c}{r}$  involved in them beforehand.

If, by some ways, the appropriate value of this factor were presumed suitably for the type of cross-section in problem, the primary computation of above formulae become possible and the buckling stress  $\sigma_a$  becomes known also, as the consequence of which we can obtain the cross-sectional area and hence, through assembling the elemental sections of rolled steels, the better value of the factor  $\frac{\eta_c}{r}$  may be got for the type of cross-section in problem. Again, starting from the latter value of the factor, the more exact values for  $\sigma_a$  and, consequently, also for the factor  $\frac{\eta_c}{r}$  itself may be obtained. Thus, through such a iteration process, we can improve the design cross-section as best we wish, and the results should converge to its exact value very rapidly. In the present research, the author intends to presume the approximate values for the factor  $\frac{\eta_c}{r}$  as follows, concerning with some types of cross-sections which are common in the bridge practice or the other steel structures.

The factor  $\frac{\eta_c}{r}$  may be analysed as

$$\frac{\eta_c}{r} = \frac{\eta_2}{h} \cdot \frac{h}{r} \dots\dots\dots(30),$$

where

- $h$  : the depth of cross-section in the plane of buckling (Fig. 3),
- $r$  : the radius of gyration in the plane of buckling.

In the bridge practice, the factor  $\frac{r}{h}$  may be admitted, approximately, as of the constant value which is peculiar to the type of cross-section. Highly efficient values of this factor have been projected upon "Structural Tables, p. 257" in "Ketchum: Structural Engineer's Handbook, 3rd edition, 1935, McGraw Hill Book Co., New York"; and for a long while, the author has used those values in teaching the design method of compression members, and also has applied in the practical design, so effectively. Thus, the author wants to adopt those numerical values as the approximate ones of the factor  $\frac{r}{h}$ , in this study.

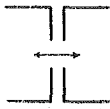
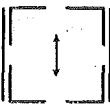

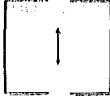

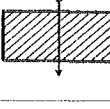
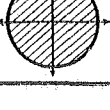
As for the other factor  $\frac{\eta_c}{h}$ , in the case of all cross-sections which are symmetrical about n-n axis, it can be put evidently as half an unity. When the cross-section is unsymmetrical about n-n axis, it is necessary to investigate about the approximate values for the factor  $\frac{\eta_c}{h}$  anew, and it is possible any way. With  $\frac{\eta_c}{h}$  known, the factor  $\frac{\eta_c}{r}$  may also be got readily. In the present treatise, these values are projected and

estimated, for some cross-sections common in the bridge practice, as follows.

(a) Cross-sections symmetrical about n-n axis.

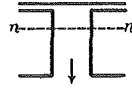
Marks ( $\longleftrightarrow$ ) or ( $\uparrow$ ) represent the direction of flexure due to the buckling.

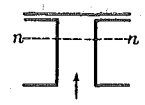
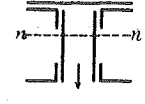
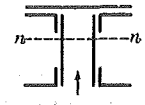
TABLE I. Factors  $\frac{\eta_c}{r}$  of symmetrical cross-sections.

Section No.	Type of Section	$\frac{r}{h}$	$\frac{\eta_c}{h}$	$\frac{\eta_c}{r}$ or $\frac{\eta_t}{r}$	Remarks
1		0.23	1/2	1/0.46	Approximate value. Section with lacing bars or tie plates; longer legs horizontal.
2		0.36	1/2	1/0.72	Approximate value. Section with lacing bars or tie plates.
3		0.21	1/2	1/0.42	Approximate value. Longer legs horizontal.
4		0.38	1/2	1/0.76	Approximate value. Section with lacing bars or tie plates.
5		0.24	1/2	1/0.48	Approximate value. Longer legs horizontal.
6		$1/2\sqrt{3}$	1/2	$\sqrt{3}$	Exact value.
7		1/4	1/2	2	Exact value. The buckling in every direction is possible.

(b) Cross-sections unsymmetrical about n-n axis.

TABLE II. Factors  $\eta_c/r$ ,  $\eta_t/r$  of unsymmetrical cross-sections.

Section No.	Type of Section	$r/h$	$\eta_c/h$	$\eta_c/r$	$\eta_t/r$	Remarks
8	Direction of a 	0.39	0.4057	1/0.961	1/0.656	Approximate value. Compressive chord

9	Direction of buckling	b		0.39	0.5943	1/0.656	1/0.961	section with lacing bars or tie plates.  Do. Longer legs horizontal
	a		0.4	0.4242	1/0.943	1/0.695		
	b		0.4	0.5758	1/0.695	1/0.943		

Values of  $\frac{\eta_c}{h}$  on TABLE II. for Section No. 8 and 9 are the averages obtained from data for Section No. 55, 73, 91, 109 and No. 155, 208, 264, 319 of "Structural Tables."

**5. Asymptotes of the buckling stresses for some cross-sections when the load ratio  $\nu^2$  will grow infinite.**

Equation (22) and (28) enables us to get asymptotic values of the buckling stresses  $\sigma_a$  and  $\sigma_{a,+}$  respectively, when the load ratio  $\nu^2$  becomes infinite. Taking as the limit of proportionality  $\sigma_p = 2100 \text{ kg/cm}^2$  for St 37 and  $3200 \text{ kg/cm}^2$  for St 52, those are computed and prepared in TABLE III.

**TABLE III** Asymptotic values of buckling stresses for St 37 and St 52 ( $\nu^2 \rightarrow \infty$ ), unit ( $\text{kg/cm}^2$ ).

Section No.	St 37		St 52		Cross-section about n-n axis	
	$\sigma_a$	$\sigma_{a,+}$	$\sigma_a$	$\sigma_{a,+}$		
2	0.272	—	0.632	—	symmetrical	
9	a	(0.4667)	0.2536	(1.083)	0.5890	unsymmetrical
	b	0.2535	(0.4671)	0.5886	(1.085)	
6	0.175	—	0.406	—	symmetrical	
7	0.131	—	0.305	—	symmetrical	

For the cases of buckling, 9a and 9b, there exists the relations between their section-factors

$$\left(\frac{\eta_c}{r}\right)_{9a} = \left(\frac{\eta_t}{r}\right)_{9b}, \quad \left(\frac{\eta_t}{r}\right)_{9a} = \left(\frac{\eta_c}{r}\right)_{9b}; \dots\dots\dots(31)$$

hence, remembering the equations (22a) and (28a), it results the following relations between their asymptotic values of buckling stresses, as numerically can be noticed on TABLE III:

$$\sigma_a(9a) = \sigma_{a,+}(9b), \quad \sigma_{a,+}(9a) = \sigma_a(9b) \dots\dots\dots(32).$$

Such two sets of equations between two modes of buckling may generally be applied for all types of cross-section from the same grade of material, which are unsymmetrical about n-n axis.

**6. Calculations and diagrams.**

Diagram 1 represents the two curves  $\frac{y_1}{l} - \nu^2$ , the one computed by the exact equation (14), the other by the approximate one (14a).

The exact maximum deflection  $\frac{y_1}{l}$  is got to be 0.4031 corresponding to  $\nu^2 = 1.749$ , while the value A. Schleusner obtained is 0.4032 for  $\nu^2 = 1.7495^*)$  According to the author's calculation, it gives the same value  $y_1/l = 0.4031$  for  $\nu^2 = 1.750$  also, and through the investigation of the effective lower decimal numerals, the author recommends  $y_1/l = 0.4031$  for  $\nu^2 = 1.749$  as the numerals for the maximum deflection. The difference between the maximum values due to exact and approximate methods amounts to about 8%.

**TABLE IV.**  $\frac{y_1}{l} - \nu^2$  values (n = 1).

$\nu^2$	$\frac{y_1}{l} - \nu^2$ values		$\nu^2$	$\frac{y_1}{l} - \nu^2$ values	
	Exact	Approximate		Exact	Approximate
1	0	0	6	0.258763	0.247
1.176	0.311655	0.299	7	0.239998	0.231
1.353	0.374921	0.352	8	0.224714	0.217
1.749	0.403108	0.373	9	0.211978	0.205
2	0.398428	0.367	10	0.201165	0.195
3	0.353544	0.328	11	0.191244	0.187
4	0.313144	0.294	12	0.183771	0.179
5	0.281850	0.268			

Diagram 2 represents the two curves  $\frac{y_1}{l} - \frac{1}{\nu^2}$ , exact and approximate. Taking the quantity  $\frac{1}{\nu^2}$  as the abscissa, the entire tendency of the relation between  $\frac{y_1}{l}$  and  $\nu^2$  becomes able to be seen throughout. Besides, by this method of representation, the slope of the curve for the region where  $\nu^2$  is small becomes less steep than Diagram 1 remarkably, the benefit which brings us in studying the curve tendency for this portion may never be accepted as so little.

\*) A. Schleusner: Strenge Theorie der Knickung und Biegung, I. Teil, S. 2), B. G. Teubner in Leipzig. u. Berlin, 1937.



Diagram 3 represents the curves  $\frac{y_1}{l} - \frac{\lambda_{c,p}}{\lambda_p} (\lambda = 99.346)$  for Sections No. 2, 9, 6, 7, of St 37. The relations  $\nu^2 - \lambda_{c,p}$  are calculated for Sections No. 2, 6, 7 by the equation (20), and for Section No. 9 by both equations (20) and (25), the one curve corresponding to the stress  $\sigma_a$  (9b) and the other to the stress  $\sigma_{a,+}$  (9a). Through the factor  $\frac{\eta_c}{r}$  or  $\frac{\eta_t}{r}$ , the type of cross-section influences the flexure of a column notably, but the magnitude of maximum deflection is constant and indifferent from varieties of the cross-section. Columns of composite section, *i. e.* No. 2 and 9, can resist the more severe bending than those of solid sections, *i. e.* No. 6 and 7, very efficiently.

Diagram 4 represents the relation  $\frac{y_1}{l} - \lambda_{c,p}$  for Sections No. 2 and 9 of St 37 ( $\sigma_p = 2100 \text{ kg/cm}^2$ ), and St 52 ( $\sigma_p = 3200 \text{ kg/cm}^2$ ). Holding the condition that the maximum fibre stress should not exceed the limit of proportionality of material, the column of St 52, as it is shown in this diagram, can resist the more intense flexure than that of St 37, with the same slenderness ratio given. For both materials, two curves corresponding to stresses  $\sigma_a$  (9b) and  $\sigma_{a,+}$  (9a) near to each other very closely.

Diagram 4a represents the same curves for the portion of the minor slenderness ratio. For both grades of materials, the area enclosed by lines abc and ae or lines ad and ae is the domain where the elastic flexure due to buckling will be possible. The area excluded from the above belongs to the domain of the plastic flexure due to buckling.

In the next place, notwithstanding the high interest for us, it is difficult to express distinctly the difference between the Euler's classical theory and the author's theory by means of tracing their curves  $\sigma_a - \lambda_{c,p}$  as usual. Such a purpose, however, may be answered supremely through plotting the curve  $\frac{\sigma_a}{\sigma_{a,E}} - \lambda_c$ , instead of the above. Diagram 5 represents these curves for cross-sections, Type No. 2, 9, 6, 7, of St 37. There, the difference of both theories becomes able to be expressed in a magnified scale. The ratio of stresses  $\sigma_a/\sigma_{a,E} (= \nu^2)$  by the Euler's and the author's theories increases very rapidly according to the growth of the slenderness ratio  $\lambda_{c,p}$ , throughout all types of cross-section. This tendency of increase is far brisker for the composite sections than for the solid ones.

Diagram 6 represents the curve  $\frac{\sigma_a}{\sigma_{a,E}} - \lambda_{c,p}$  for Sections No. 2 and 9, considering as the material both St 37 and St 52 for each cross-section. The positive deviation of the author's theory from the Euler's is more active for the material of higher

grade, St 52, than the lower one, St 37, as shown in the diagram; namely, the grade of material influences the critical stress of elastic buckling of a steel column remarkably, and its influence grows active increasingly accompanied with the growth of the slenderness ratio. Two curves for  $\sigma_a$  (9b) and  $\sigma_{a,+}$  (9a) are coincident approximately for the portion of the major slenderness ratio for both grades of materials, and the buckling stress for the cross-section Type No. 9 is less than that for Type No. 2 for the portion of the major slenderness ratio.

Diagram 7 represents the same curve with Diagram 6, for the minor slenderness ratio. For both materials, St 37 and St 52, two curves subject to the buckling stresses  $\sigma_a$  (9a) and  $\sigma_{a,+}$  (9a), have their intersection points, which correspond to  $\nu^2 = 1.000534$ ,  $\lambda_{c,p} = 257$  for St 37, and  $\nu^2 = 1.000807$ ,  $\lambda_{c,p} = 207$  for St 52. For the portion of  $\lambda_{c,p}$  major to the intersection point, the buckling law  $\sigma_{a,+}$  (9a) is responsible, and for the minor one, the law  $\sigma_a$  (9a), each expressing the lesser value than the other. Both bucklings subject to stresses  $\sigma_a$  (9a) with  $\lambda_{c,p}$  major to this intersection point and  $\sigma_{a,+}$  (9a) with  $\lambda_{c,p}$  minor to the same point are impossible on the elastic region, because, if these were possible, the extreme fibre stress on the tensile or on the compressive side should exceed the limit of proportionality of material respectively, which will convert the buckling plastic. The curve subject to the buckling law  $\sigma_a$  (9b) indicates itself as the minimum of the three sorts of curves, and consequently, this law can be accepted as provided with a technical significance for a column of Section No. 9. The law  $\sigma_{a,+}$  (9a) becomes imaginary for the portion minor to the point  $\nu^2 = 1.000242$ ,  $\lambda_{c,p} = 90.358$  for St 37, and  $\nu^2 = 1.0003705$ ,  $\lambda_{c,p} = 80.494$  for St 52.

For the purpose of proving these values, we substitute the relation

$1/\phi^2(\nu) = \frac{E}{4\sigma_p} \left(\frac{\eta_l}{r}\right)^2$  into the equation (25), and get

$$\lambda_{c,p} = \pi \sqrt{\frac{E}{\sigma_p}} \nu = \nu \lambda_p \tag{33}$$

which corresponds to the slenderness ratio of the terminal point of the real region where the buckling stress  $\sigma_{a,+}$  is possible, and this equation gives the values mentioned above with  $\nu^2 = 1.000242$  or  $1.0003705$  for St 37 or St 52 respectively. This value of  $\lambda_{c,p}$  nears  $\lambda_p$  very closely, but is slightly greater than  $\lambda_p$ .

The difference between  $\sigma_a/\sigma_{a,b}$ -values subject to the buckling stresses  $\sigma_{a,+}$  (9a) and  $\sigma_a$  (9b) is greater for the portion of the minor and lesser for the portion of the major slenderness ratio  $\lambda_{c,p}$ , the relation  $\sigma_{a,+}$  (9a)  $\geq$   $\sigma_a$  (9b) being held always. Their values, however, can be seen nearly coincident for the entire range of slenderness ratio and its difference which is slight originally becomes lesser and lesser when the slenderness ratio grows greater, to which a caution should be exercised.

Comparing curves for Sections No. 2 and 9, the buckling stress for the former section is always greater than the stress  $\sigma_n$  (9b) for the latter one; compared with the stress  $\sigma_{a,+}$  (9a), though it is greater than this stress for the portion of the major slenderness ratio, Diagram 6, it becomes lesser than this for the portion of the minor one, Diagram 7; it is, also, less than the buckling stress  $\sigma_n$  (9a) for the portion where the slenderness ratio is minor to the intersection point b in Diagram. 7. Through above observations of diagrams, we may define as the domain of elastic buckling taking Section 9 for an example, the area bounded between the lines abc and ae for the mode of buckling 9a, and the area bounded between the lines ad and ae for the mode of buckling 9b (Diagram 7), each having an infinite range of its scope accompanied with the growth of the slenderness ratio  $\lambda_{c,p}$ . There, the classical theory of Euler makes the lower limiting boundary of the domain of elastic buckling, ae, and the author's one provides the upper limiting boundary of the same domain, abc or ad. The area excluded from this ought to be no other than the domain of plastic buckling. These circumstances and tendencies are all to be understood distinctly upon Diagrams 6 and 7.

If we denote the bending stress of a column with  $\sigma_b$ , the fundamental criterion of elastic buckling gives the relation

$$\frac{\sigma_b}{\sigma_a} = \frac{\sigma_p}{\sigma_n} \mp 1, \text{ (positive sign for } \sigma_{a,+}) \dots\dots\dots (34)$$

which expression enables us to observe the relative variation of bending and direct stresses, both being constituents of the resultant fibre stress which should amount to the stress  $\sigma_b$  at the limit of elastic buckling. Diagram 8 represents such curves,  $\frac{\sigma_b}{\sigma_a} - \lambda_{c,p}$ , for symmetrical and solid Sections 6 and 7 of St 37 and St 52. This ratio increases actively with the growth of slenderness ratio at first, and as this slenderness ratio grows greater, however, braking this tendency, the curve  $\frac{\sigma_b}{\sigma_a}$  approaches his asymptote which is peculiar to the type of cross-section and the grade of material. The proportion responsible to the bending stress is heavier for Section 7 than for Section 6, throughout the slenderness ratio and the grade of material. Related about the grade of material, the above proportion is heavier for St 52 than for St 37 where a column is provided with the minor slenderness ratio, and, is heavier for St 37 than for St 52 where the major slenderness ratio prevails, both indifferently from the type of cross-section.

Diagram 9 represents the curves similar with Diagram 8, for Sections 2 and 9 of St 37 and 52. The tendency of increase is just the same with above mentioned about Diagram 8.

Namely, for the region of the slenderness ratio major to 7800 for Section 2 and 8080 for Section 9, (cases of  $\sigma_a$  (9b) and  $\sigma_{a,+}$  (9a)), the ratio  $\sigma_b/\sigma_a$  for St 37 are greater than for St 52, and vice versa. For both grades of material, two curves for  $\sigma_a$  (9b) and  $\sigma_{a,+}$  (9a) almost coincide each other throughout total range of the slenderness ratio, excepting the region of the minor one, cf. Diagram 9a also. The proportion responsible to the bending stress is heavier for Section 9 than for Section 2, throughout the slenderness ratio and the grade of material.

Diagram 9a represents the curve  $\sigma_b/\sigma_a$  for the region of the minor slenderness ratio, concerning materials St 37 and St 52. With the exception of the case  $\sigma_{a,+}$  (9a), the values of this ratio subject to the stresses  $\sigma_a$  (9a),  $\sigma_a$  (9b), and  $\sigma_a$  (2) are all coincident almost perfectly in such a region of the slenderness ratio, while for stresses  $\sigma_a$  (9b) and  $\sigma_{a,+}$  (9a) are also coincident for the region of the major slenderness ratio, as we have observed on Diagram 9, these being, there, greater than the ratio for the stress  $\sigma_a$  (2). Indifferently from the types of cross-section, the stress ratio  $\sigma_b/\sigma_a$  is always greater for St 52 than for St 37 upon this diagram.

Diagram 10 represents the variation of the stress ratio  $\sigma_u$  (St 52)/ $\sigma_a$  (St 37) due to the slenderness ratio  $\lambda_{c,n}$ , for both cross-section Type 2 and 9. For the region of the minor slenderness ratio, the effect of the grade of material is negligibly small, while it grows active for the region of the major one, indifferently from types of the cross-section; when the slenderness ratio becomes greater and greater, it approaches gradually to its asymptote. This asymptotic value amounts to about 2.322 for both types of the cross-section, which shows the maximum value of the effect due to the grade of material. For the region of the major slenderness ratio, the stress ratios based upon  $\sigma_a$  (9b) and  $\sigma_{a,+}$  (9a) coincides approximately, while they are fairly less than the ratio for Section 2. The asymptotic values of the stress ratio are provided with no differences approximately for the cases of buckling stresses  $\sigma_a$  (2),  $\sigma_a$  (9b) and  $\sigma_{a,+}$  (9a), which nearly amount to the square of the ratio from the limit of proportionality for both grades of material, as can be understood from formulae (22a) and (28a).

Diagram 10a represents the curves similar with Diagram 10 for the region of the minor slenderness ratio. Though the grade of material has, as a whole, a very slight effect upon the elastic buckling stress for the region of such a slenderness ratio, we can still recognize fair differences of the grade effect, due to the mode of buckling and the type of cross-section. Deviating from the tendency as observed in Diagram 10 for the region of the major slenderness ratio, the stress ratio for  $\sigma_a$  (2) becomes, in this case, notably lesser than for  $\sigma_{a,+}$  (9a), while it is still greater than for  $\sigma_a$  (9b), though it nears the latter curve so closely. The stress ratio for  $\sigma_a$  (9a) shall be effective for the range of the slenderness ratio from 99,346 to 207,

which indicates greater values than for  $\sigma_{a,+}$  (9a) corresponding to the region of the slenderness ratio major to about 163, and vice versa; it is, however, impossible and ineffective for the region of the slenderness ratio major to 207, which is expressed in a dotted line in this diagram, cf. Diagram 7. also.

## 7. Conclusions

It may be mentioned some important conclusional remarks from the preceding results, as follows.

1. For the region of the slenderness ratio major to  $\lambda_p = \pi \sqrt{\frac{E}{\sigma_p}}$ , certainly, there exists the domain of the elastic buckling, where we can apply more column load than the Euler's, his buckling theory  $\sigma_{a,E} = \frac{\pi^2 E}{\lambda^2}$  making the lower limiting boundary of this domain, while the author's, the upper one of the same, and due to a concentric load applied beyond the Euler's critical one an arbitrary elastic buckling is possible upon the domain bounded by and between both theories. This upper limiting boundary is peculiar to the grade of steel material and the type of cross-section. The stress ratio  $\sigma_e/\sigma_{a,E}$  to be obtained by both theories increases actively accompanied with the growth of the slenderness ratio, and, at the extremity, to an infinity. Hitherto it was considered that, when the column stress exceeds the Euler's critical one, immediately there follows a plastic buckling\*,) but according to the author's theory the column can resist to the stress far greater than  $\sigma_{a,E}$  in the elastic buckling when the slenderness ratio is major, though the former conception is true just at the critical slenderness ratio  $\lambda_p$ , and, also, approximately true for the slenderness ratio near by  $\lambda_p$  (Diagrams 5, 6, 7).

2. All the curves of the upper limiting boundaries peculiar to the types of cross-section converge simultaneously to the point of the stress  $\sigma_p$  at the critical slenderness ratio  $\lambda_p$ , which correspond to the maximum buckling stress and the minimum slenderness ratio of the domain of the elastic buckling respectively. This slenderness ratio amounts to 99.346 for St. 37 and 80.479 for St 52 (Diagram 7, the points a).

3. The Euler's classical theory instructs, as the influence factor of the material, the modulus of elasticity solely, while the present theory has found that, besides, this factor, the limit of proportionality of the material  $\sigma_p$  effects a firm influence upon the strength of the elastic buckling, *i. e.*, approximately in the square of it. Thus, acknowledging the existence of the remarkable influence of the grade of

\*) As an example of such a far-reaching thought, it may be quoted: Swain: Structural Engineering (Strength of Materials), p. 426, 1924, McGraw Hill, New York, N. Y.

material, the theory of the elastic buckling has become to be provided with its reasonableness and perfectness, and consequently the proper significance and contents of the elastic buckling has become to be understood distinctly through such a theory, at the first time (Diagram 4, 6, 7).

4. According to the Euler's theory, the column can resist no load at its slenderness ratio of an infinity, while the author's theory instructs the fact that such a column with an infinite slenderness ratio is still able to resist a load of some finite value, though it is small. In the other words, it necessitates still to apply some finite load, surely, in order to make the maximum fibre stress introduced in such a long column equal to the limit of proportionality of the material. This asymptotic value of the elastic buckling stress is peculiar to the grade of material and the type of cross-section (TABLE III).

5. The column of St 52 can resist the more intense flexure than that of St 37 elastically (Diagram 4, 4a). Hence, the limiting stress of the elastic buckling,  $\sigma_a$ , is far greater for St 52 than for St 37, and this positive effect of the grade of material increases remarkably with the growth of the slenderness ratio (Diagram 6, 7). And the stress ratio  $\sigma_a$  (St 52)/ $\sigma_a$  (St 37), finally, converges to the asymptotic value of the square ratio of the limits of proportionality of both materials approximately, namely 2.322, which value is nearly indifferent from the type of cross-section (Diagram, 10, 10a). Thus, we can recognize the fact that the higher grade of material enlarges the domain of the elastic buckling notably, on account of heaving the upper limiting boundary stress and lowering the critical minimum slenderness ratio  $\lambda_n$ , of the domain in problem.

6. The influence of the grade of material upon the elastic buckling strength of a column is fairly different according to the type of cross-section. Taking the cases of Sections 2 and 9, as an example (Diagram 10, 10a), we can observe no such a notable difference of this influence between them for the region of the minor slenderness ratio. Nevertheless, for the region where the slenderness ratio becomes major, the difference of the grade effect upon the cross-section type grows fairly great; and with the slenderness ratio grown greater furthermore, the above difference becomes slight again, and the stress ratio  $\sigma_a$  (St 52)/ $\sigma_a$  (St 37) for each cross-section type converges to the asymptotic value 2.322 (approximate) gradually. The type of Section 2 may be acknowledged to be far sensible than that of Section 9 for the influence due to the grade of material.

7. For the columns with the same moment of inertia but the different cross-section types, the Euler's theory shall give the same buckling stress  $\sigma_{a,E}$ , while the author's theory gives, in this case, the different buckling stresses, because the new

theory involves, besides the moment of inertia, the quantity  $\frac{r}{\eta_c}$  or  $\frac{r}{\eta_t}$  as the factors of the cross-section, by the square of the latter one the buckling stress  $\sigma_u$  being influenced approximately, and hence, making the effect of the cross-section type remarkable (Diagram 5). The similar effect of the cross-section type upon the flexure of the column may be accepted as remarkable also (Diagram 3). Furthermore, we know that the composite section is superior to and more effective than the solid section in the resistance to the intense flexure and stress due to the elastic buckling always, with the exception of the types of Sections, 1,3 and 5, *i. e.*, the I-type cross-sections (Diagram 3, 5). Among the composite types, the I-type cross-sections are of little advantage at the standpoint of the elastic buckling, because their cross-section factors  $\frac{r}{\eta_c}$  are all less than those of the solid sections (TABLE I).

8. The column of the symmetrical cross-section has a single mode of the elastic buckling for the entire range of the slenderness ratio. In the case of an unsymmetrical cross-section, the double modes of the same are possible for the region of the major slenderness ratio, though the limiting buckling stresses  $\sigma_u$  subject to them are closely near by each other (Diagram 6). For the region of the minor slenderness ratio, the triple modes of the same are possible, their limiting buckling stresses rather being of little differences as a whole. Three modes of the buckling of the latter case, however, are never possible simultaneously for the given slenderness ratio, but it is possible in pairs of two modes of the same for the definite regions of the slenderness ratio which are different from each other (Diagram 7). Namely, taking the case of Section 9 as an example, the mode of the buckling subject to the stress  $\sigma_u$  (9b) is possible for the entire range of the slenderness ratio, while the curves of the buckling modes  $\sigma_u$  (9a) and  $\sigma_{u,+}$  (9a) have an intersection point in the region of the minor slenderness ratio, the mode  $\sigma_{u,+}$  (9a), hence, being possible for the region of the slenderness ratio major to this point, and the mode  $\sigma_u$  (9a) possible for the same ratio minor to the same point, elastically. And such a tendency may be valid always in the case of an unsymmetrical cross-section, invariably from the grades of material (Diagram 7).

9. Regardless of the grade of material, it is advantageous to design the unsymmetrical composite cross-section so as to make factors  $r/\eta_c$  and  $r/\eta_t$  equal, as the result of which the buckling stresses subject to the double modes of buckling approach to each other, thus heaving the upper limiting boundary of the domain of elastic buckling to be determined by the disadvantageous mode of buckling (as an example, the case  $\sigma_u$  (9ba) in Section), Diagram 7. For the case of the symmetrical composite cross-section, with the sectional area given, it is advantageous to design

the cross-section to be provided with the larger values of the factors  $\frac{r}{\eta_c}$  for both orthogonal directions of the symmetrical axes (biaxial case), and this is invariable also for the monoaxially symmetrical cross-section.

10. The component bending stress  $\sigma_b$  of the resultant maximum fibre stress which reaches at the stress  $\sigma_b$  at the limit of the elastic buckling increases so rapidly with the growth of the slenderness ratio, compared relatively with the average column stress  $\sigma_u$ , that, taking as an example Section 9, the difference between the buckling stress  $\sigma_u$  (9b) and  $\sigma_{u,+}$  (9a) subject to the double modes of elastic buckling almost vanishes for the region of the major slenderness ratio (Diagram 9). Consequently the stress ratio  $\sigma_b/\sigma_u$  also increases actively accompanied with the growth of the slenderness ratio, and it approaches gradually to the asymptote which is peculiar to the cross-section type and the grade of material. In spite of the varieties of the cross-section type, this asymptotic value for St 52 is lesser than for St 37 by 34.4% simultaneously, the reason of which lies upon the fact, that, for the region of the major slenderness ratio, the portion responsible to the stress  $\sigma_u$  is far greater for St 52 than for St 37, while for the region of the medium slenderness ratio, vice versa. For the solid cross-section, the same portion is far lesser than for the composite cross-section type (Diagram 8, 9). Finally, excepting the case of  $\sigma_{u,+}$  (9a), the differences among the stress ratios  $\sigma_b/\sigma_u$  due to the types of cross-section may almost vanish for the region of the minor slenderness ratio, and the ratio values become to form a single curve approximately (Diagram 9a).

11. For the practical region of the minor slenderness ratio (in bridge practice,  $\lambda < 200$ ), there should be no essential impediment approximately in the design of a compression member to follow the classical theory of Euler,  $\sigma_{a,E} = \frac{\pi^2 E}{\lambda^2}$ .

12. Finally, the author wants to inspect the permissible deflection of a long column which is to be expected for the elastic buckling. In the Japanese bridge practice, the permissible maximum slenderness ratio for the grade of structural steel is specified as 150 for laterals and sway bracings, and 200 for the composite tension members, which values can be sought to correspond to the permissible deflections mentioned in TABLE V, applying Diagram 4a. Those values are obtained for Sections 2 and 9, as the difference of which for the two types of cross-section is very small for such a region of the slenderness ratio; the case of the larger buckling stress  $\sigma_u$  (9a) is excepted here.

By this table, we know that a fairly great flexure due to the elastic buckling is admitted in this country. The column from the higher grade of material may have an ample margin allowance to the limit of elastic buckling, holding the same



buckling flexure with the lower grade one.

**TABLE V.** Permissible deflection  $y_1/l$  of Japanese Specification for Bridges  
(Type Sections 2 and 9)

$\lambda$	$y_1/l$	
	St 37	St 52
150	$0.0058 \pm 1/172$	$0.0115 \pm 1/87$
200	$0.0106 \pm 1/94$	$0.0180 \pm 1/56$

### Postscript

The incomplete abstract of the treatise was sent to Chairman Prof. Dr. Ingr. K. Yuasa to be submitted to the general meeting of Column Research Committee of Japan, J. S. C., 4. May, 1949, some parts of which related to the buckling strength of the column of an unsymmetrical cross-section has been improved afterwards and made complete by the author as delivered in the present one. Hence, he is liable to express that some parts of the former diagrams and conclusions mentioned there, relating to the above item, should have been modified reasonably as to be seen in this treatise.

The author gratefully acknowledges his indebtedness to Mr. Y. Maeda and Mr. T. Yoshino for assisting in calculations and the drafting of diagrams.

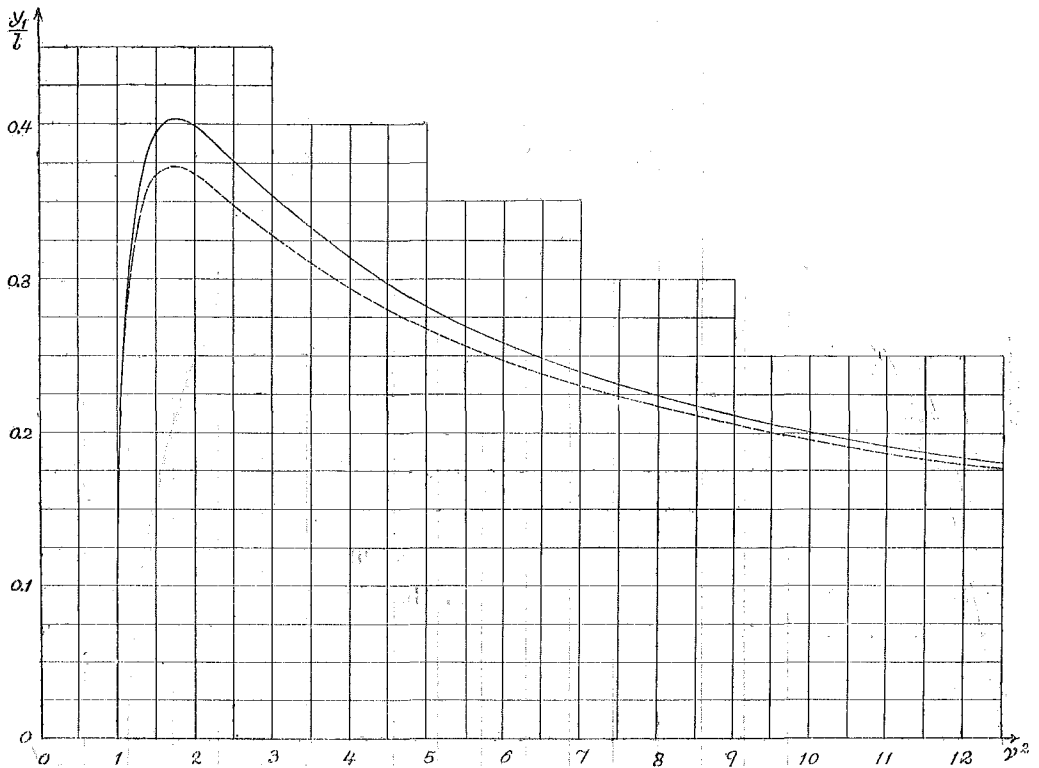
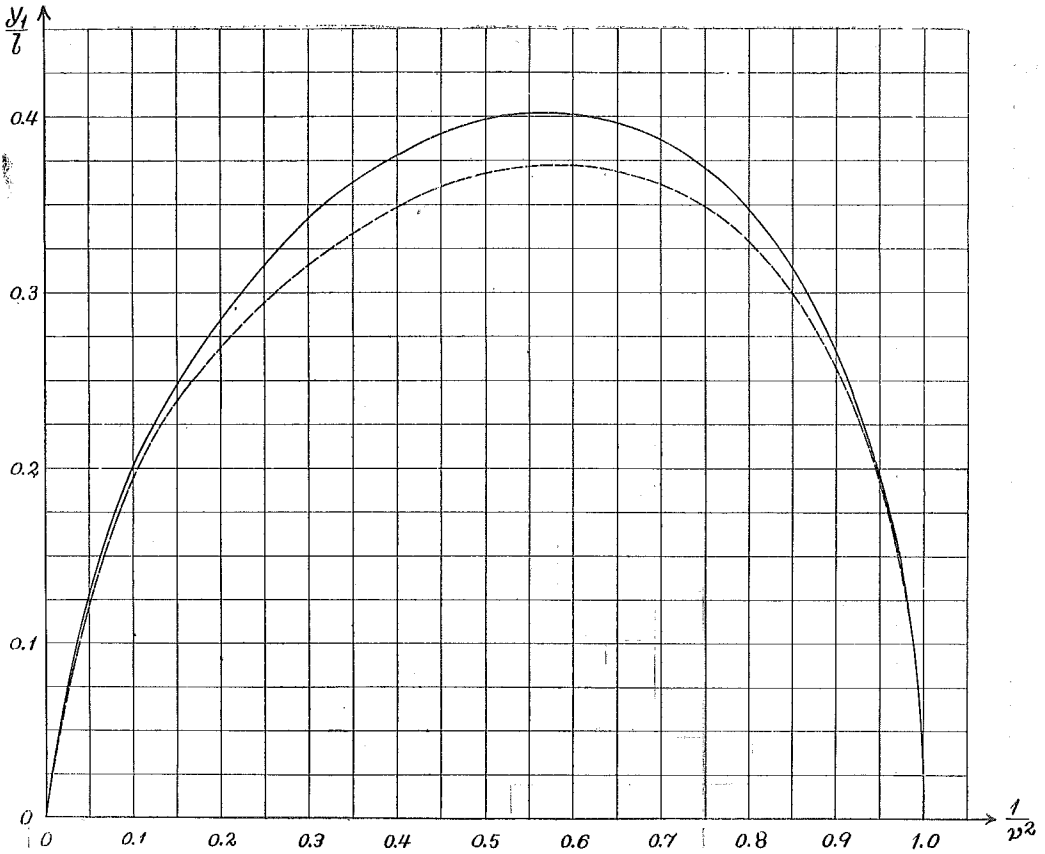


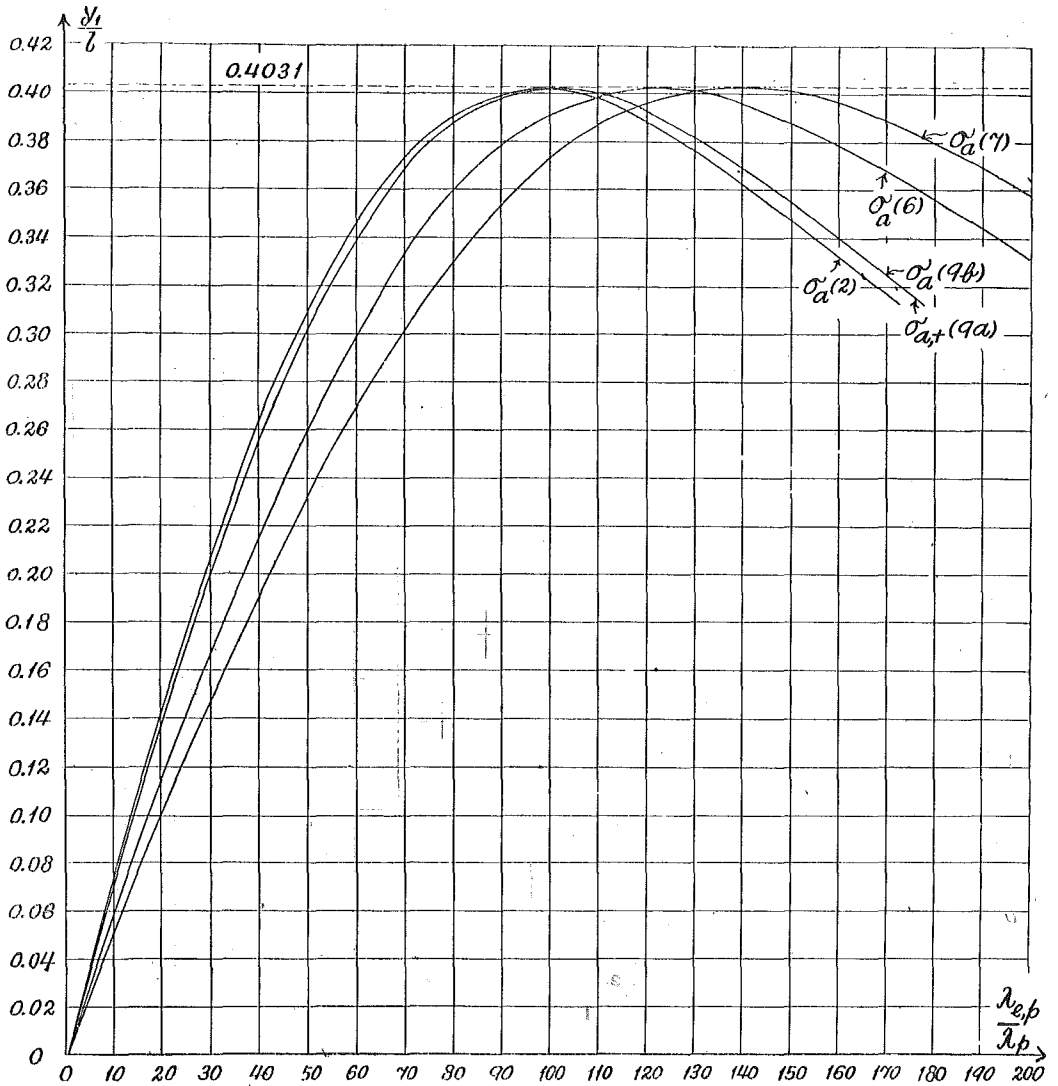
Diagram I. Curve of Center Deflection

Full line: Exact curve.

Dotted line: Approximate curve.



**Diagram 2.** Curve of Centre Deflection  
Full line: Exact curve.  
Dotted line: Approximate curve.



**Diagram 3.** Curves of flexure for various cross-section Types of St. 37. Numbers in brackets denote Types of cross-section and Modes of buckling (cf. TABLES I, II, III)

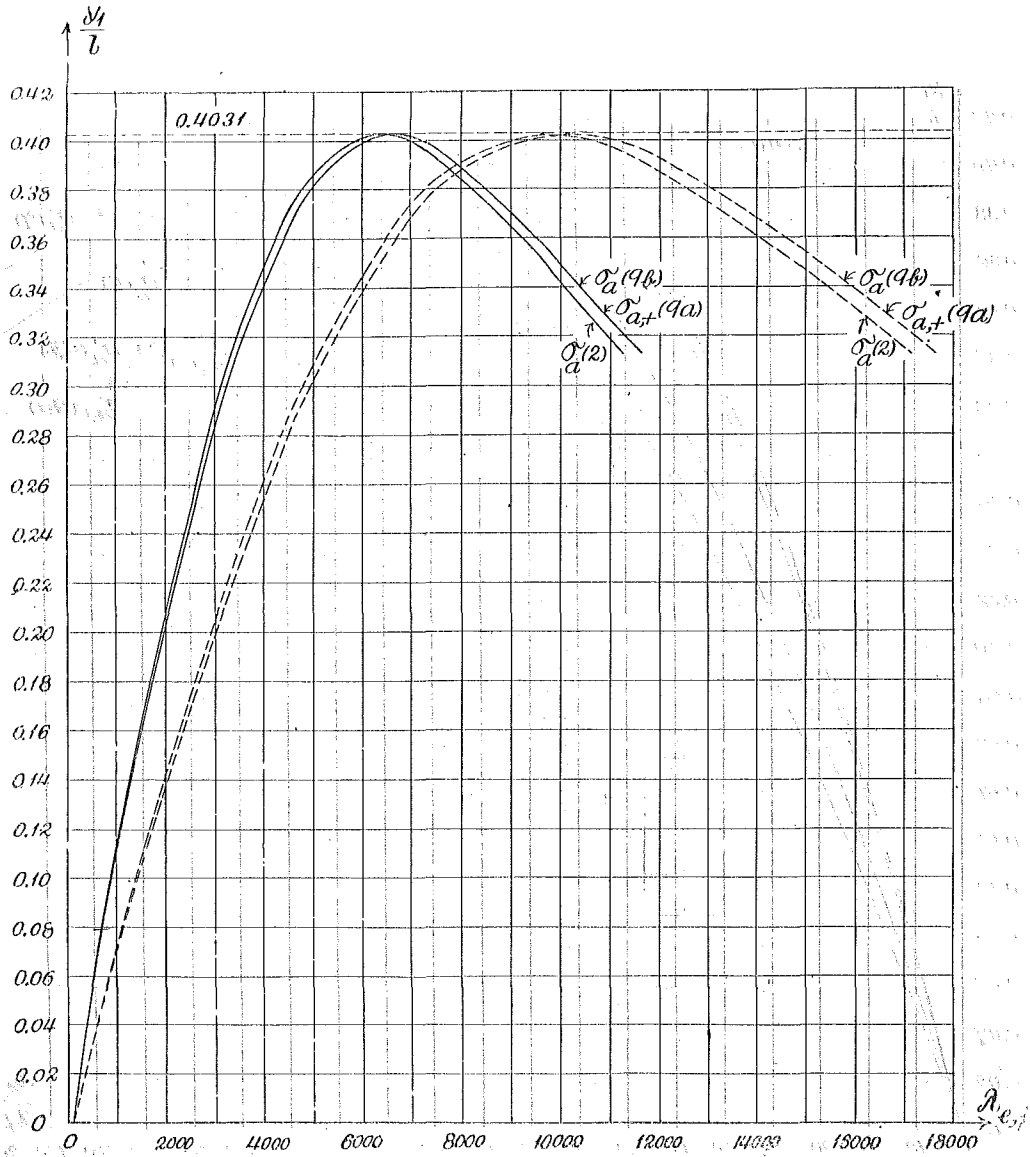


Diagram 4. Curves of flexure for St 52, and St 37, Sections 2 and 9.

Full line: St 52

Dotted line: St 37

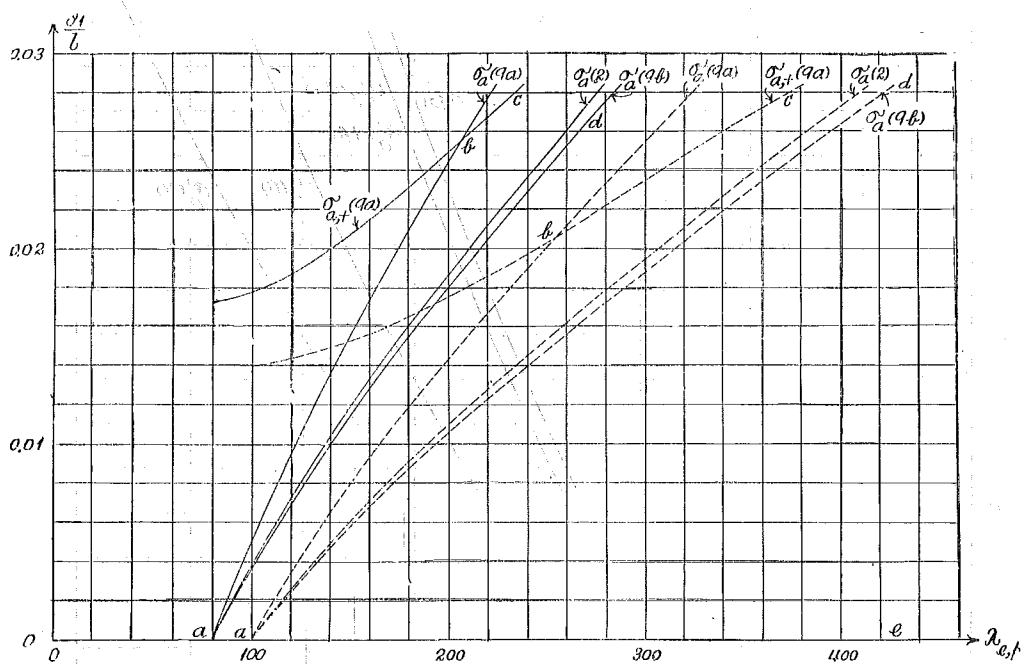
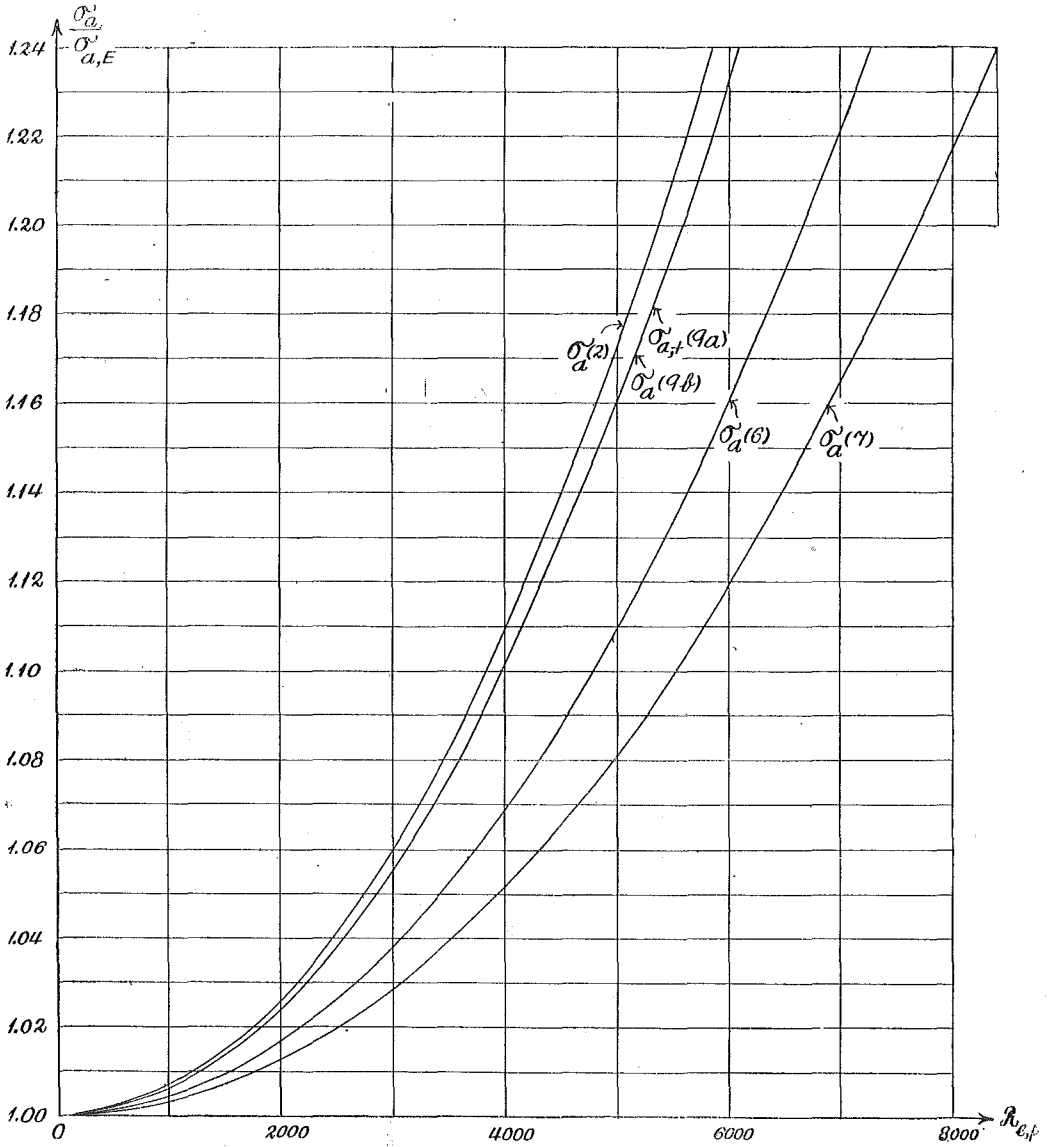


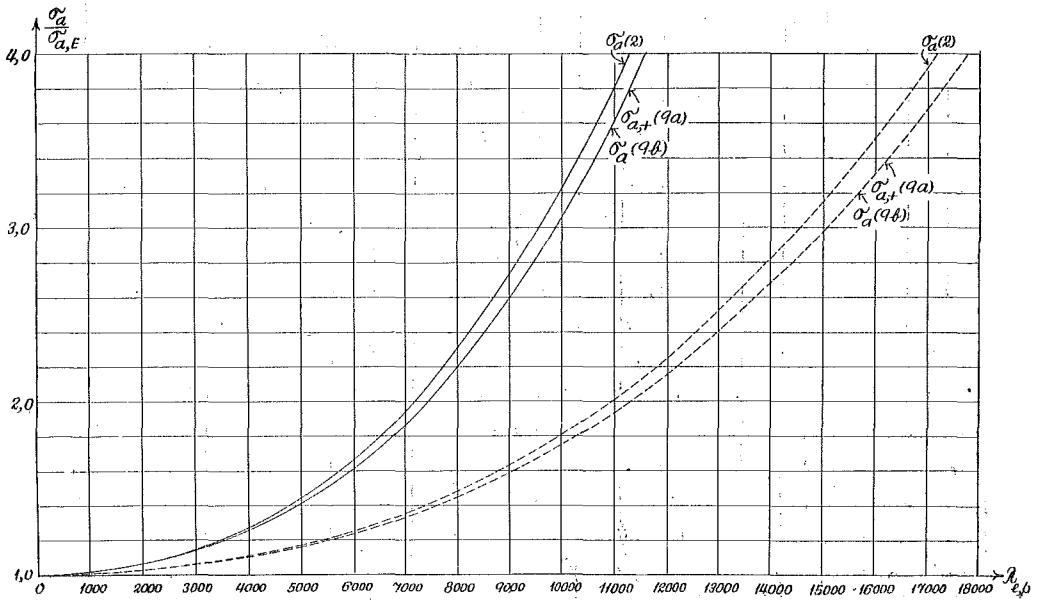
Diagram 4a. Curves of flexure for the minor slenderness ratio.

Full line: St 52

Dotted line: St 37



**Diagram 5.** Curves  $\sigma_a/\sigma_{a,E} - \lambda_{c,D}$  for St 37.  
 Numbers in brackets denote Types of cross-section and Modes of buckling (cf. TABLES I, II III).



**Diagram 6** Curves  $\sigma_a / \sigma_a E - \lambda_{e,p}$  for St 52 (Full lines) and St 37 (Dotted lines).  
Types of cross-section: 2 and 9.



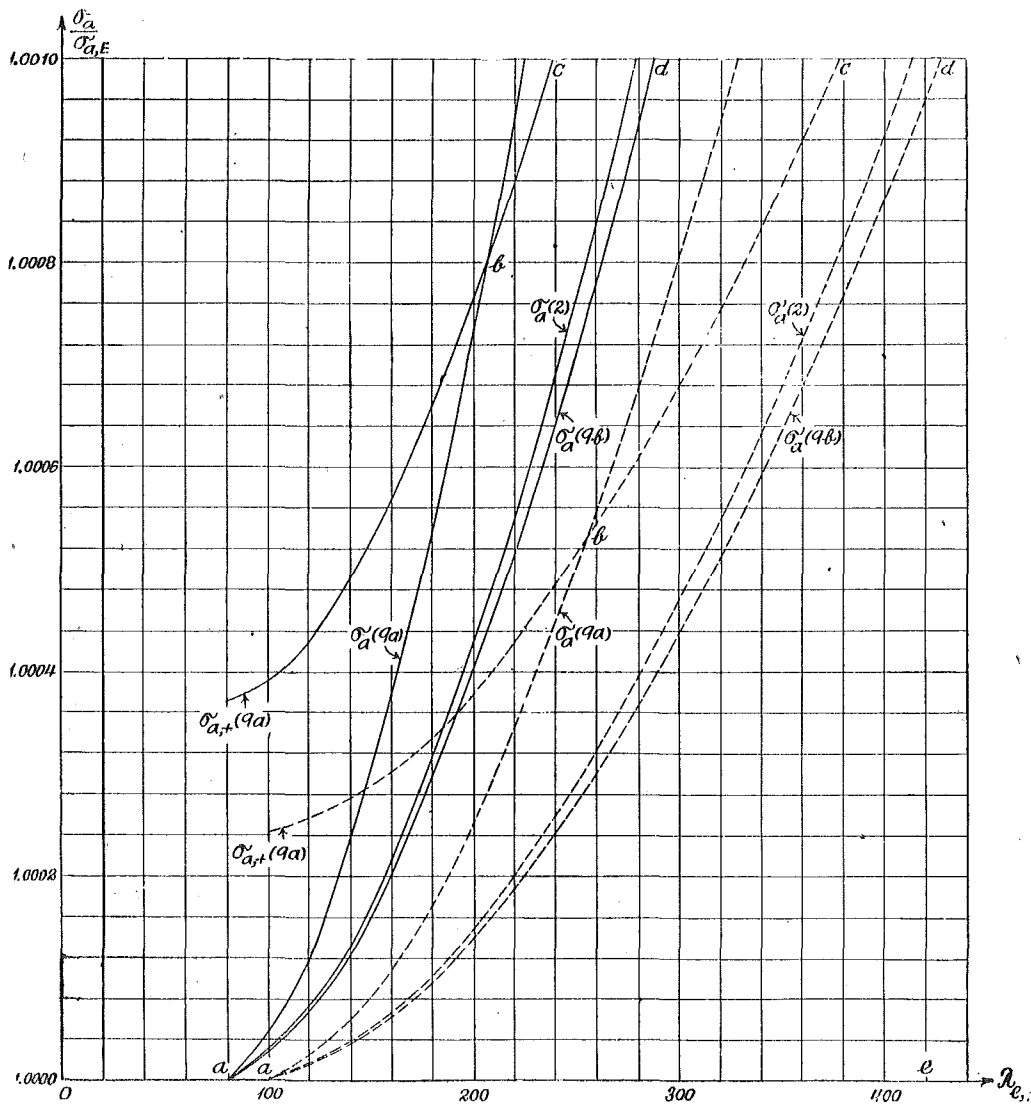


Diagram 7. Curves  $\sigma_a/\sigma_{a,0} - \lambda_{e,0}$  for the minor slenderness ratio.  
Materials: St 52 (Full lines) and St 37 (Dotted lines).

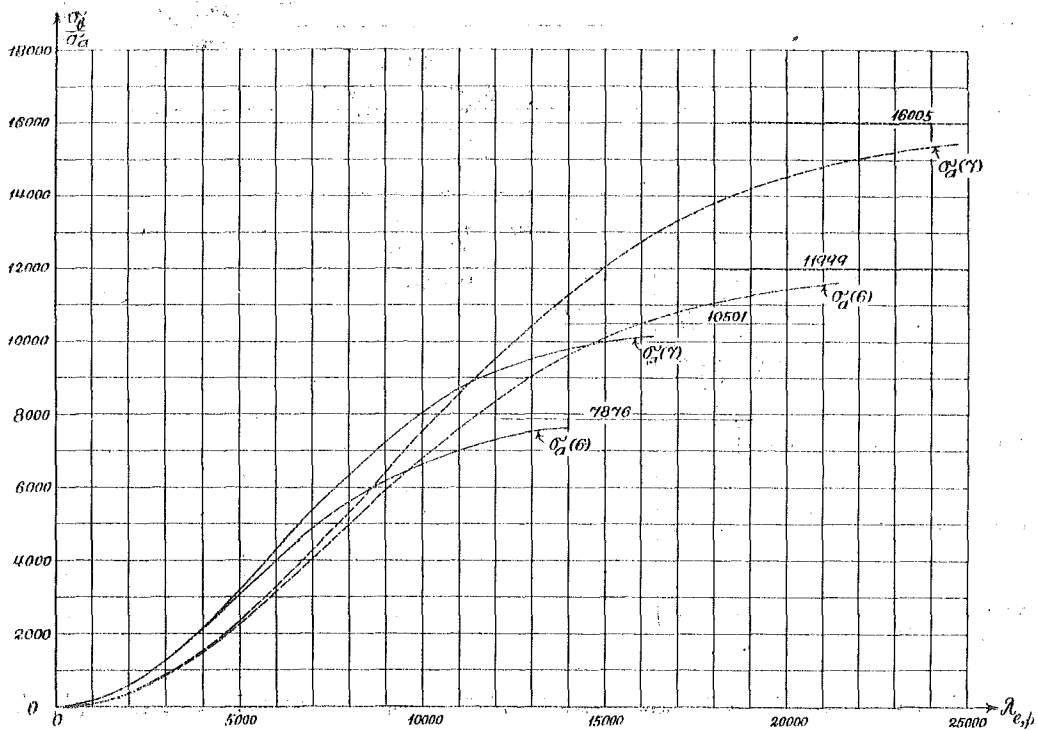


Diagram 8. Curves  $\sigma_b/\sigma_a - \lambda_{e,p}$  for Sections 6 and 7.

Materials: St 52 (Full lines) and St 37 (Dotted lines).

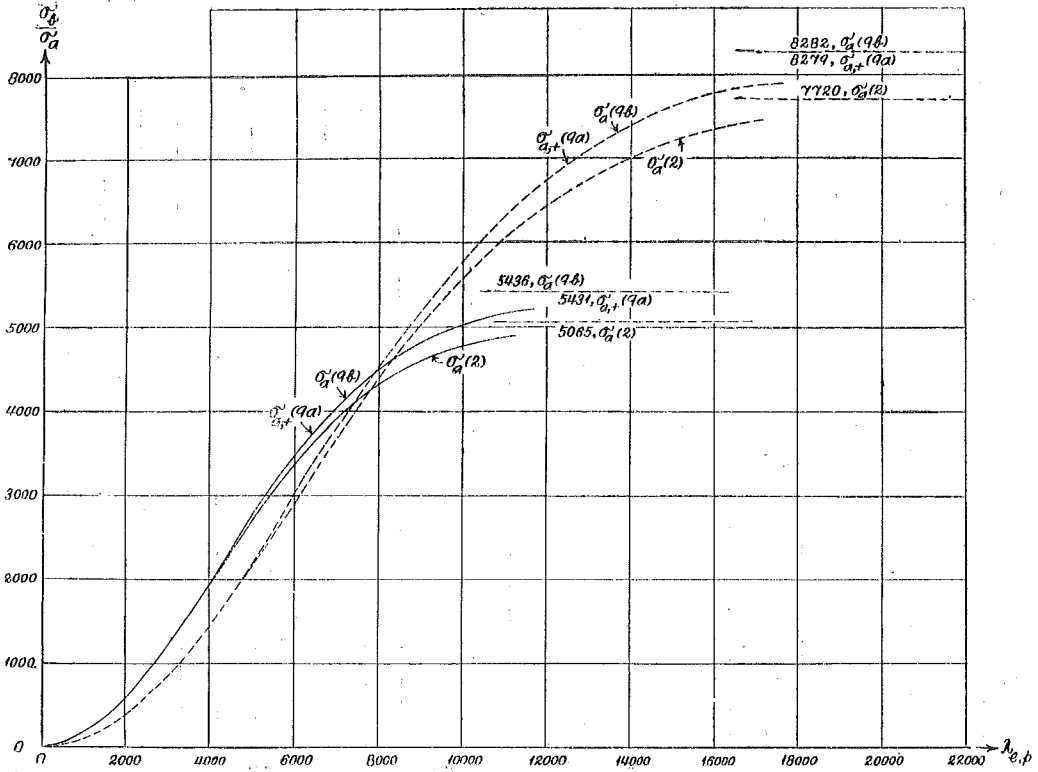
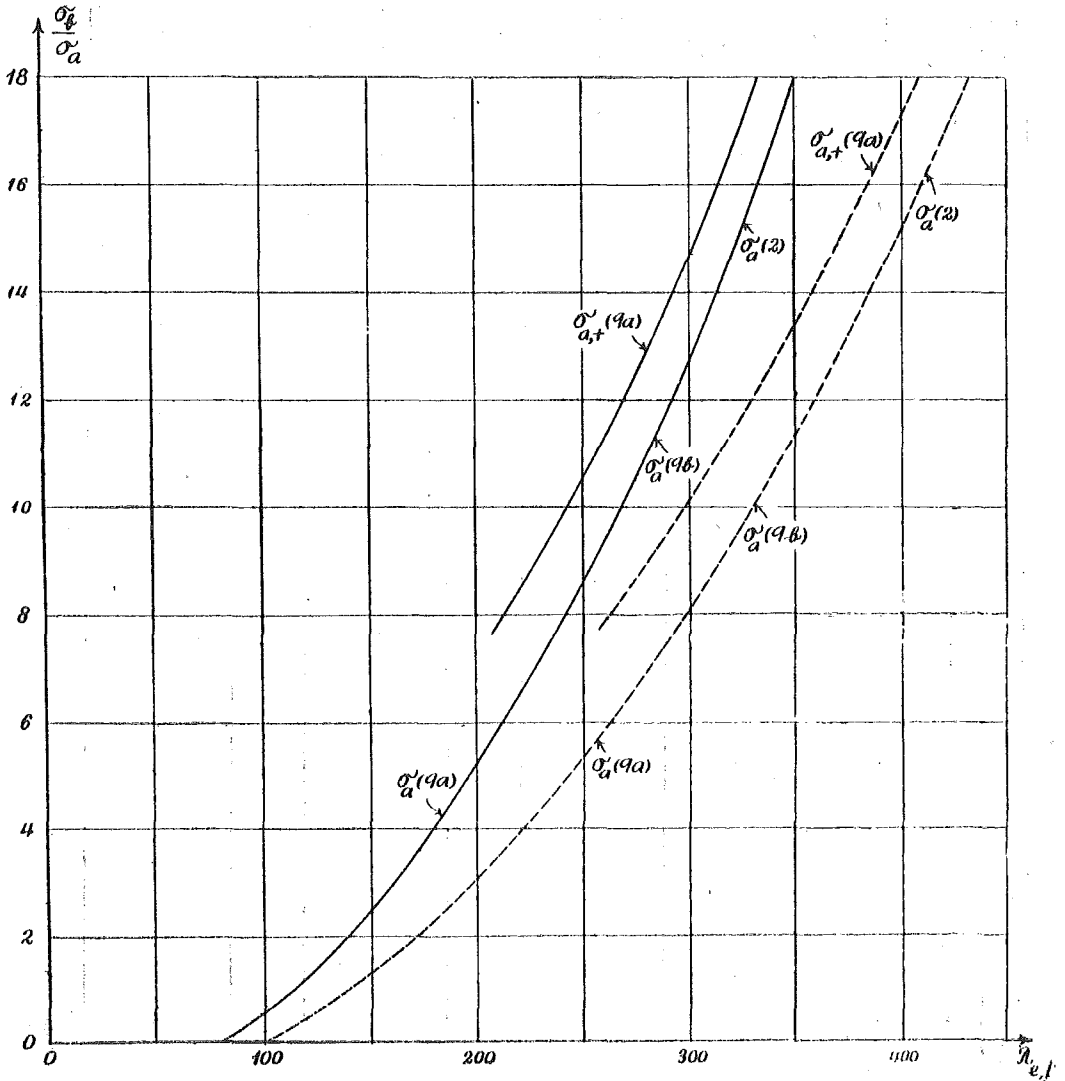


Diagram 9. Curves  $\sigma_p/\sigma_a - \lambda_{e,p}$  for Sections 2 and 9.

Materials: St 52 (Full lines) and St 37 (Dotted lines).



**Diagram 9a.** Curves  $\sigma_c/\sigma_a - \lambda_{e,y}$  for the minor slenderness ratio,  
 Sections 2 and 9.  
 Materials: St 52 (Full lines) and St 37 (Dotted lines).

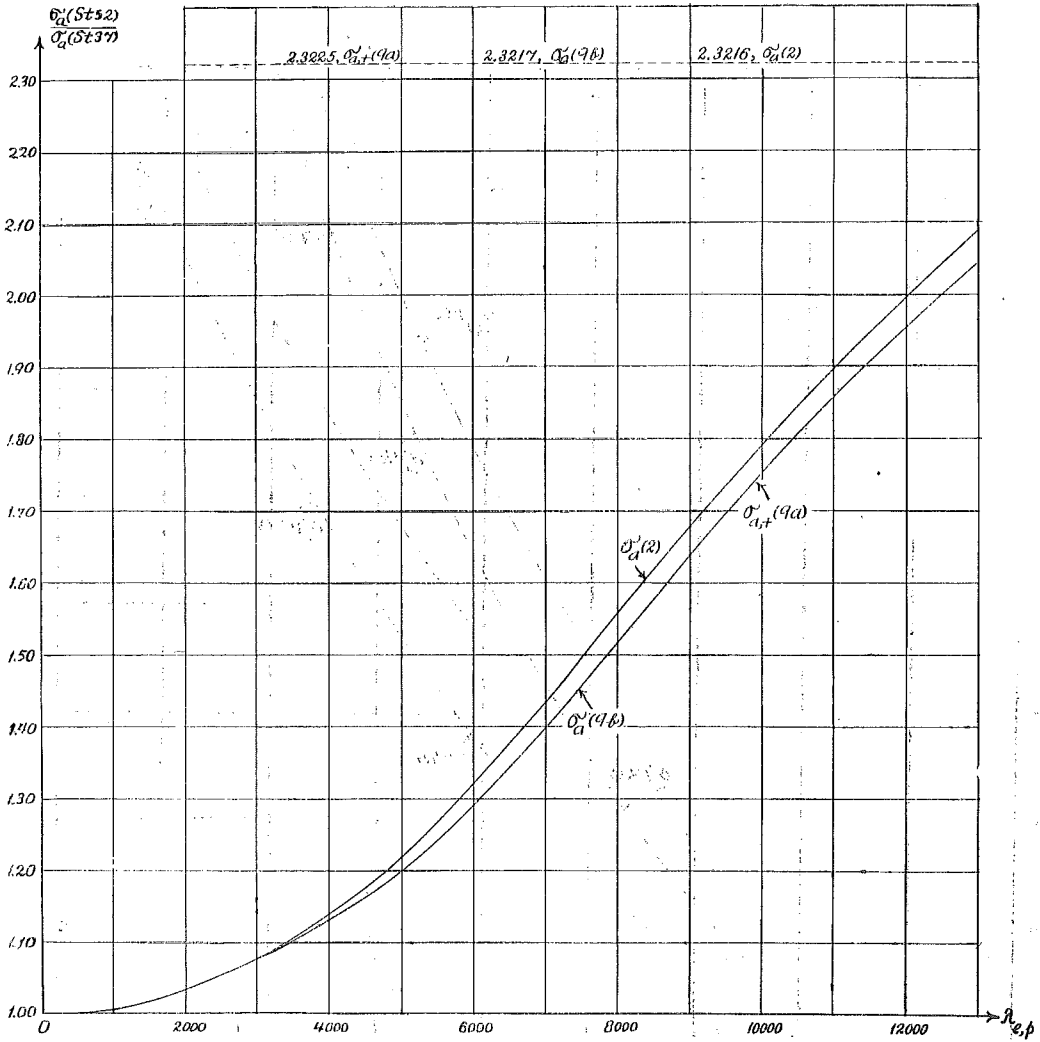


Diagram 10. Curves  $\sigma_a$  (St 52)/ $\sigma_a$  (St 37) for Sections 2 and 9.

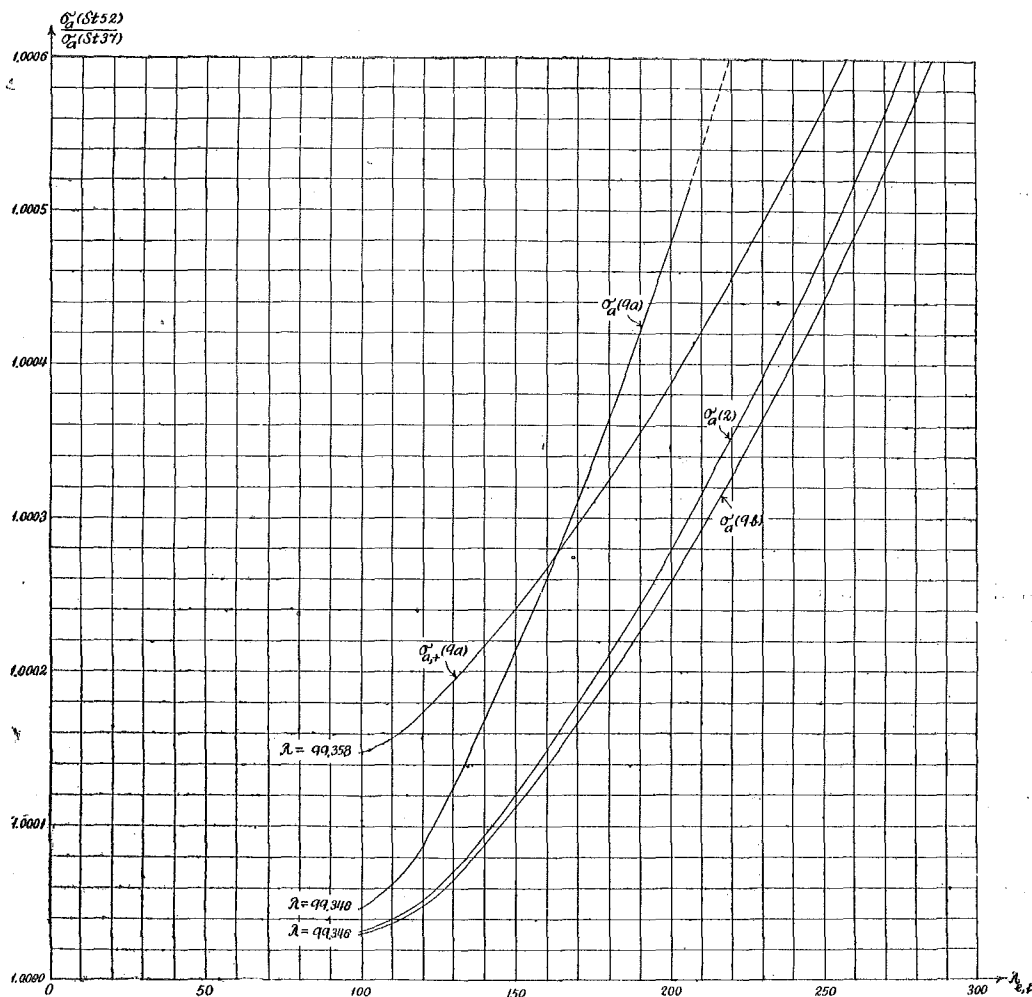


Diagram 10a. Curves  $\sigma_a(\text{St } 52) / \sigma_a(\text{St } 37)$  for the minor slenderness ratio, Sections 2 and 9.